Journal of Mammary Gland Biology and Neoplasia (2025) 30:13
https://doi.org/10.1007/s10911-025-09589-1

BRIEF REPORT

MaGNet: A Network-Based Method for Quantitative Analysis of the Mammary Ductal Tree in Developing Female Mice

Steven M. Lewis[1,2,3] · Lucia Tellez-Perez[1,4] · Samantha Henry[1] · Xingyu Zheng[1,4] · Saket Navlakha[1] · Camila O. dos Santos[1]

Received: 7 April 2025 / Accepted: 13 August 2025

Abstract

The mammary gland is a uniquely dynamic organ with a branching architecture that develops entirely after birth in response to hormonal cues. A common approach in mammary gland biology is the evaluation of branching morphogenesis to characterize the role of developmental, physiological and molecular perturbations on branching tissue invasion, growth, and maintenance. Yet, the field still lacks a fully open-sourced, quantitative framework to analyze whole-mount mammary tissue images, as a commonly utilized methodology. Here, we present MaGNet (*Ma*mmary *G*land *Net*work analysis tool), a method that leverages network theory to characterize key features of ductal branching during mammary gland development. Applying this pipeline to mammary gland images captured at three pubertal timepoints, we achieved reproducible quantification of ductal tree expansion across development. In addition, this network analysis pipeline captures ductal expansion induced by pregnancy hormones. By providing open-source tools to the research community, this method may increase reproducibility and broad applicability across diverse organ systems, model organisms, and developmental stages.

Main Text

Branching is a fundamental morphogenic pattern found in life across plants and animals at the tissue and cellular level [1, 2]. In plants, branching occurs at the level of shoots and in the veins of leaves (alongside the branches from which the name of the structural pattern is derived) [3, 4]. In animals, branching morphogenesis occurs during the development of organs as varied as the kidney, liver, lung, pancreas, prostate as well as at the cellular level in the dendrites of neurons and in the antigen presenting dendritic cell of the innate immune system [5].

Unlike most other organs, the mammary gland in female mice undergoes the majority of its branching morphogenesis postnatally, driven by hormonal cues associated with puberty [6]. In mice, this pubertal transition—marked by a rise in circulating estrogen—typically occurs between 4 and 7 weeks of age and initiates the outgrowth and elongation of the mammary ductal tree [7]. Whole-mount imaging of mammary glands during this developmental window reveals striking structural changes, including expansion of the ductal epithelium throughout the fat pad and, in some models, the early emergence of malignant lesions [8–11]. Therefore, the quantifying of ductal branching initiation and elongation has emerged as a key approach for assessing how molecular or cellular perturbations influence mammary gland expansion across developmental stages [5, 12]. Despite its critical importance, the field still lacks a robust and widely adoptable method for quantifying mammary gland morphology that delivers consistent reproducibility across both normal development and neoplastic transformation studies.

Previous advances in network theory-based analysis of ductal branching morphogenesis have been largely built on entirely manual pipelines with custom made software or convoluted imaging modalities such as optical projection

Steven M. Lewis, Lucia Tellez-Perez and Samantha Henry contributed equally to this work.

✉ Camila O. dos Santos
dossanto@cshl.edu

[1] Cold Spring Harbor Laboratory, NY 11724 Cold Spring Harbor, USA

[2] Graduate Program in Genetics, Stony Brook University, NYStony Brook, USA

[3] Medical Scientist Training Program, Stony Brook University, NYStony Brook, USA

[4] School of Biological Sciences, Cold Spring Harbor Laboratory, NY 11724 Cold Spring Harbor, USA

Published online: 26 September 2025

tomography scanning [5, 13–16], [16]. However, these approaches often lack open-source availability and typically require specialized expertise to operate. These limitations underscore the need for an accessible analysis pipeline that is scalable, user-friendly, reproducible, and easily adaptable, thus offering a practical alternative to closed, and technically demanding methods. Here, we present a method of Mammary Gland Network Analysis (MaGNet), a validated, user-friendly, and freely available method for the quantification of branching morphogenesis from 2D whole-mount mammary gland images, using a network theory–based computational approach.

The MaGNet method leverages the conceptual framework of network theory to quantitatively and systematically analyze the mammary ductal tree. Within this framework, networks represent the structural organization of the gland, where nodes correspond to branch points or terminal end buds (TEBs), and edges represent the ducts connecting them (Fig. 1). By abstracting the ductal architecture into a graph of undirected and unweighted edges, we simplify the analysis without compromising accuracy. While this model currently emphasizes macro-level branching dynamics, it is readily adaptable for future integration of edge directionality or weights—features that could capture physiological parameters such as nutrient flow, ductal thickness, or spatial-temporal remodeling (Fig. 2). This approach provides a powerful, flexible platform to interrogate mammary gland morphology across diverse developmental and disease contexts.

To convert whole-mount mammary gland images into analyzable network graphs, we utilized the previously validated tool NEFI (Network Extraction From Images) [17]. This tool is particularly well-suited for the analysis of mammary gland whole mount, as its ductal architecture inherently forms a branching network. After tracing and extracting the network structure from the images, we processed the data using the Python-based NetworkX package [18]enabling high-throughput and customizable quantitative analyses (Fig. 3A–J). The resulting network models allow for automated computation of key architectural metrics, including total node and edge counts, node degree distributions, and the identification of terminal nodes (Fig. 4A–F). While the image tracing step currently involves manual user input, all downstream analyses are fully automated, thus supporting reproducibility, scalability, and broad applicability across experimental conditions.

As a proof of principle, we applied the MaGNet analytical pipeline to analyze whole-mount mammary gland

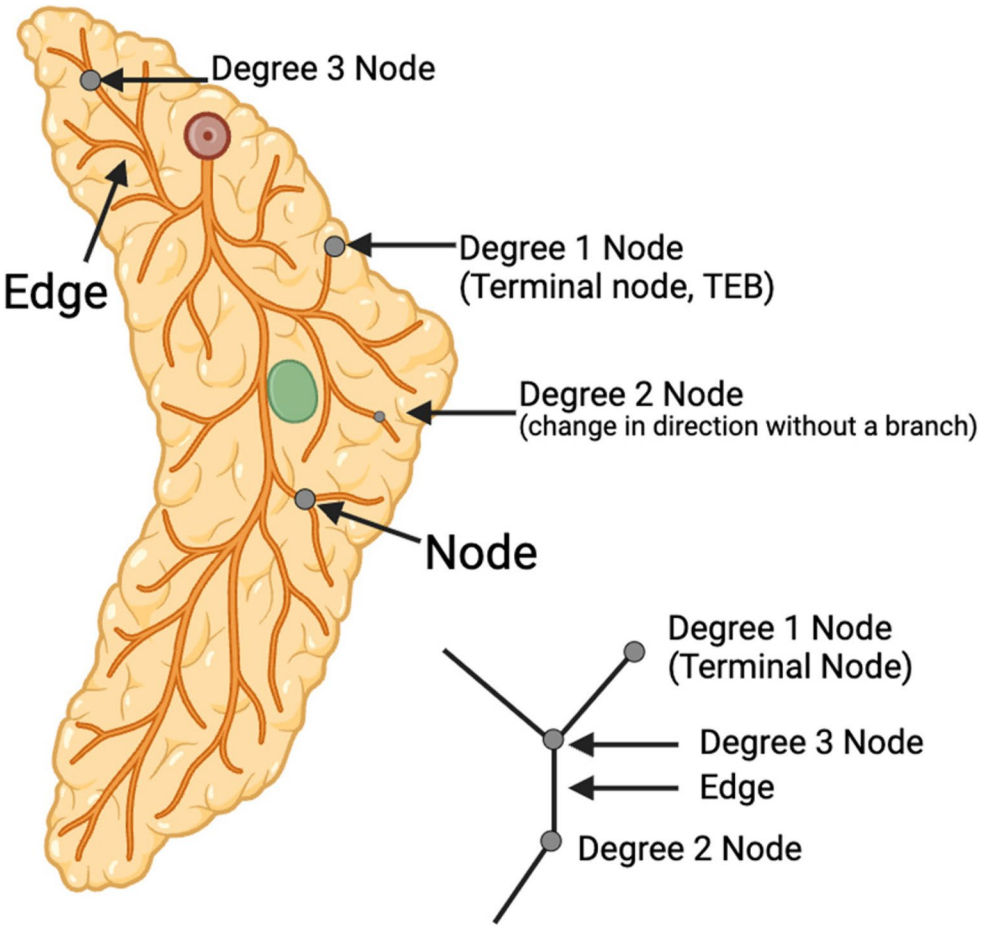

Fig. 1 Illustration of a mammary ductal tree network, and how it compares to a network schematic, with features such as nodes, edges, terminal nodes and degree noted

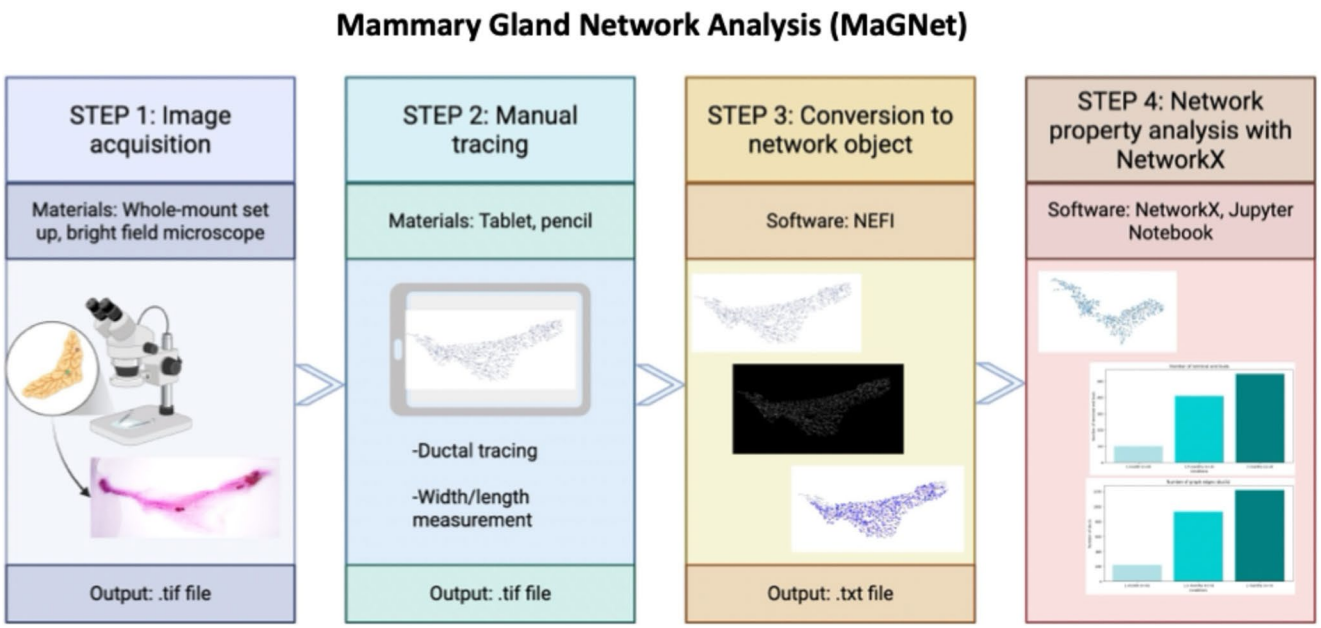

Fig. 2 Schematic overview of MaGNet analysis pipeline, beginning with brightfield image acquisition and manual tracing of the mammary ductal tree, followed by conversion of the traced structure into a NEFI-compatible format for downstream network analysis using NetworkX

images from wild-type female mice at three closely spaced developmental stages, 1 month, 1.5 months, and 2 months of age, thus capturing the critical window of pubertal onset (Fig. 4A–C). These timepoints were strategically selected to test the sensitivity of our method in detecting rapid, hormone-driven changes in ductal morphogenesis. Our network-based quantification revealed statistically significant increases in key architectural features of the ductal tree, including a ~ 4-fold rise in the number of nodes (branch points/TEBs, 4.19-fold), edges (ducts, 4.23-fold), and terminal nodes (branches, 4.06-fold) in mammary glands from 1.5-month-old female mice compared to those at 1 month of age. These results demonstrate the MaGNet pipeline's robustness in detecting short-term but significant morphogenic changes during this developmental window (Fig. 4D-H).

Comparative analysis of mammary ductal networks between 1.5- and 2-month-old female mice revealed modest but statistically significant differences in tissue architecture. Specifically, we observed a ~ 1.3-fold increase in nodes (branch points/TEBs), edges (ducts), and terminal nodes (branches) in the 2-month-old samples relative to 1.5-month-old counterparts (Fig. 4D–H). These findings indicate a developmental shift from rapid ductal expansion to structural refinement and maturation during late puberty, dynamics that were effectively captured by the quantification method offered by MaGNet.

The MaGNet quantification pipeline also facilitates high-resolution analysis of node degree distributions across diverse physiological and experimental contexts. In our developmental dataset, we observed a consistent pattern in which approximately 50% of branching nodes displayed either a degree of 1 (terminal) or 3 (bifurcation), independent of animal age. This finding underscores a stereotypical bifurcating architecture of the mammary ductal network during pubertal development (Fig. 4I). Nodes with a degree of 2, indicative of direction changes without branching, were rarely detected, suggesting that ductal outgrowth proceeds with high directional fidelity during this developmental window. Yet, the number of nodes with degree 1 (terminal) and degree 3 (bifurcation) rose markedly during the pubertal phase of mammary gland development, with a ~ 4-fold increase observed between 1- and 1.5-month-old mice, and a further 1-fold increase from 1.5 to 2 months (Fig. 4J). Collectively, these quantifications are consistent with known developmental dynamics of puberty and mammary gland morphogenesis [13]. Our observations demonstrate the MaGNet pipeline's sensitivity in capturing both rapid ductal expansion during early puberty and the subsequent refinement phase characterized by more subtle remodeling of the mammary architecture.

To further demonstrate the versatility and sensitivity of the MaGNet pipeline across distinct developmental contexts, we also analyzed whole-mount mammary gland images from a previously published study in which nulliparous wild-type mice were treated with slow-release estrogen and progesterone pellets to mimic pregnancy-induced mammary gland development [8]. We specifically compared ductal tree architecture at 6- and 12-days following hormone exposure. MaGNet analysis of traced images revealed

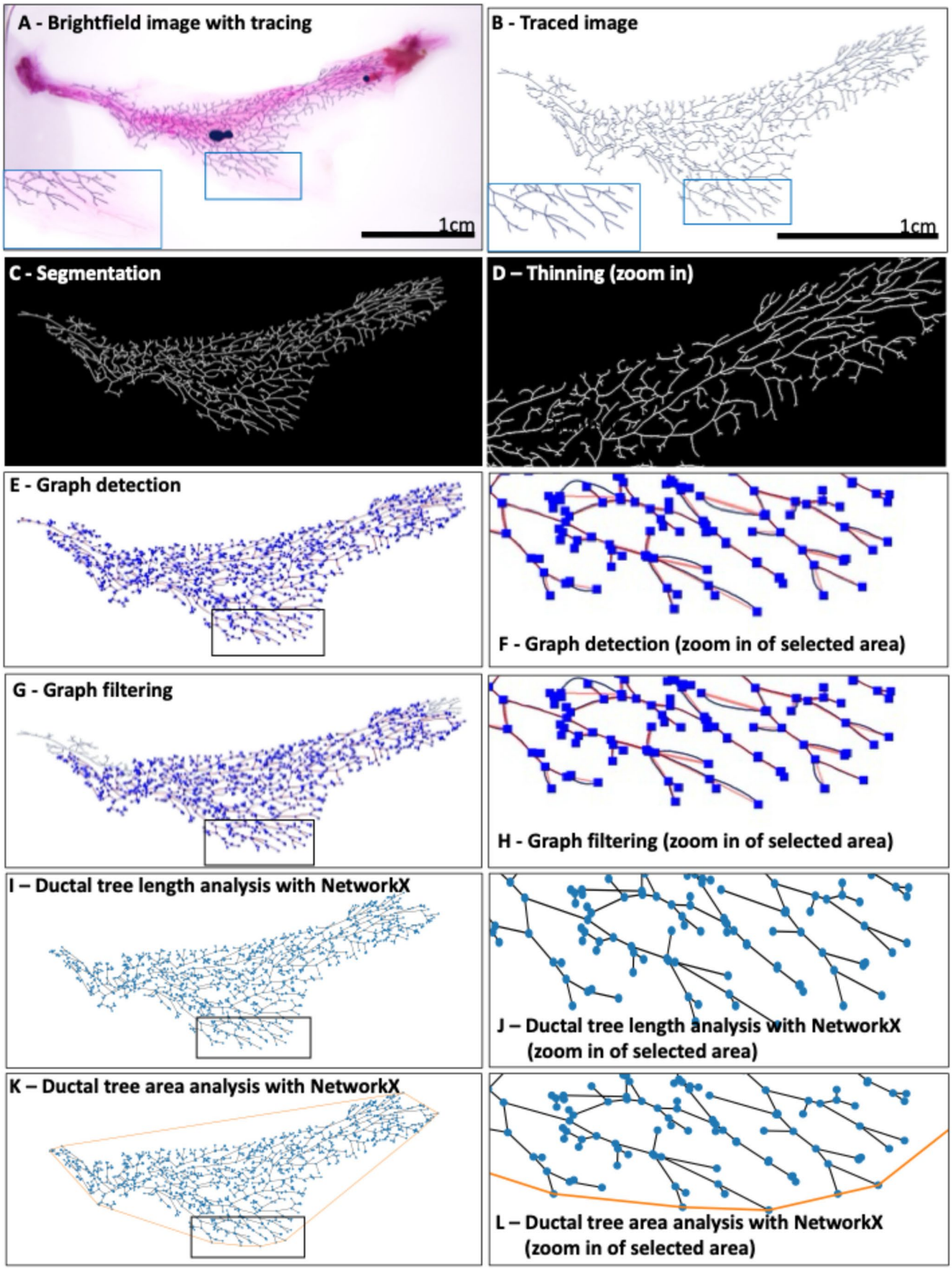
A - Brightfield image with tracing
1cm
B - Traced image
1cm
C - Segmentation
D – Thinning (zoom in)
E - Graph detection
F - Graph detection (zoom in of selected area)
G - Graph filtering
H - Graph filtering (zoom in of selected area)
I – Ductal tree length analysis with NetworkX
J – Ductal tree length analysis with NetworkX
(zoom in of selected area)
K – Ductal tree area analysis with NetworkX
L – Ductal tree area analysis with NetworkX
(zoom in of selected area)

Fig. 3 Processing from mammary gland whole mount images using MaGNet pipeline. **A** Acquisition of brightfield images of whole-mount staining. **B** Conversion to a tracing manually. **C-H** Conversion of the tracing into a NEFI object using segmentation (**C**), thinning (**D**), graph detection (**E-F**) and filtering (**G-H**). All NEFI steps are shown as a zoom-in for image clarity (**D, F, H**). **I-L** Analysis of the network graph using a NetworkX object. A representative NetworkX object is shown with its derived total ductal tree length (**I-J**), and ductal tree area (area within the network limits) (**K-L**). The functionalities to calculate ductal tree length and area are included in our open-source code

marked increases in key structural metrics, including a 1.6-fold rise in branch points (nodes), a 1.6-fold increase in ductal segments (edges), and a 1.6-fold elevation in terminal branches by day 12 compared to day 6 (Fig. 5A–C). These results highlight MaGNet's capacity to capture hormone-driven morphogenic changes with high resolution, reinforcing its utility in quantifying dynamic remodeling of the mammary epithelium during simulated pregnancy.

To assess the methodological reproducibility and robustness of MaGNet, we compared quantifications across users and additional conventional methodologies. Analysis of inter-user quantification variability was evaluated by having three independent users manually trace three separate mammary gland samples (1-month-old), followed by automated network analysis. Although slight variations were observed, the quantification of terminal nodes identified across users were not statistically significant, suggesting consistency of the tracing quantification in a user-independent manner (Fig. 6A).

To further evaluate the performance of the MaGNet pipeline, we compared its network-based quantification outputs with conventional manual duct counts obtained from H&E-stained mammary tissue Sects. [19–22]. While the comparison did not yield statistically significant differences in absolute duct counts, MaGNet demonstrated greater sensitivity in detecting sample-to-sample variation. This suggests that MaGNet provides a more consistent assessment of ductal features that are often underrepresented or missed in manual quantification approaches (Fig. 6B-D). These findings underscore the utility of MaGNet in offering a more nuanced and scalable alternative to traditional histological analysis.

Overall, our analysis and conclusion support that the MaGNet pipeline offers a valuable and accessible resource for the mammary gland development research community. In addition to its robust mode of quantification, the MaGNet pipeline is fully available as an annotated Colab Notebook, which contains all necessary steps for conducting a mammary quantification network-based analysis. The code is modular and easily adaptable to accommodate user-specific datasets or experimental designs. While image tracing remains a technically demanding step and could be viewed as a current limitation of MaGNet, this platform establishes a foundational framework that is readily compatible with future integration of automated tracing tools. Such advancements are expected to significantly improve both the usability and reproducibility of the quantification workflow, further enhancing its value to the research community. Importantly, the MaGNet pipeline is compatible with the NetworkX Python package [18]enabling users to extend the analysis beyond basic metrics like nodes and edges to include advanced topological features such as centrality, clustering coefficients, and path lengths. These capabilities position the MaGNet pipeline as a scalable and customizable platform for quantitative analysis of mammary ductal architecture, while providing a robust and extensible alternative for whole mount mammary quantification.

Materials and methods

Animals

Wildtype C57BL/6 female animals of 1 month, 1.5 and 2 months of age were used in this study and ordered from Charles River. For hormone exposure experiments, Balb/C female mice (6–8 weeks old) were ordered from Charles River [8]. All experiments involving mice were completed in agreement and approval by the CSHL Institutional Animal Care and Use Committee.

Whole-Mount Staining

After dissection of the lower left mammary gland from mice, the gland was spread carefully on a glass slide and the protocol followed as previously described [8]. In brief, the mammary gland was fixed overnight at 4 °C with Carnoy's fixative (3 parts 100% ethanol, 1 part glacial acetic acid). Post fixation, the Carnoy's fixative solution was discarded, and the mammary glands were incubated in 70% ethanol for 15 min, following wash with running tap water for 5 min. Mammary tissue was then stained with Alum carmine solution (1 g Carmine dye, 2.5 g potassium alum, MilliQ water to 500 mL, filtered) for at least 24 h at 4 °C, following a serial 15 min washes with ethanol solution at 70%, 95%, and 100% (each repeated once). Stained and washed mammary tissue was then immersed in histoclear solution overnight or until the fatpad has cleared, followed by imaging. For long-term slide storage, mammary tissue slides can be mounted with permount and stored at room temperature shielded from light.

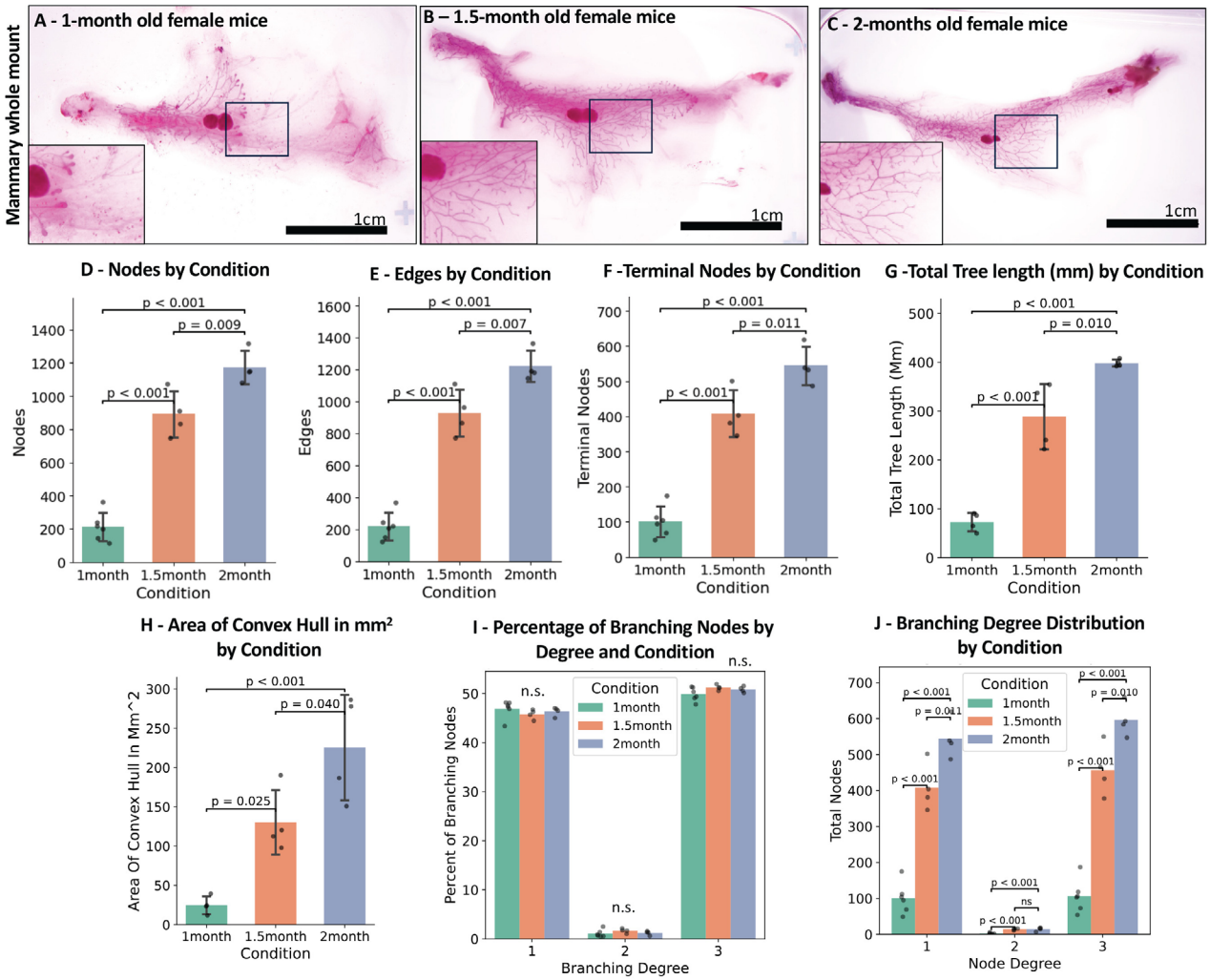

Fig. 4 Utilization of MaGNet for the quantification of whole-mount mammary gland images during pubertal development. **A-C** Representative whole-mount images at the three studied timepoints. **D-F** Quantification of the number of nodes (**D**), ductal branching tree (**E**), and terminal nodes (**F**), from mammary tissue obtained from female mice at 1 month old ($n=6$), 1.5 months old ($n=4$) and 2 months old ($n=4$). **G** Quantification of the total tree length (mm) by Condition from 1 month ($n=4$), 1.5 months ($n=4$) and 2 months ($n=4$) old female animals. **H** Quantification of area of convex hull (mm [2]) by Condition from 1 month ($n=4$), 1.5 months ($n=4$) and 2 months ($n=4$) old female animals. **I** Quantification of percentage of branching nodes by degree and condition from 1 month ($n=6$), 1.5 months ($n=4$) and 2 months ($n=4$) old female animals. n.s. = not statistically significant. **J** Quantification of branching degree distribution by condition from 1 month ($n=6$), 1.5 months ($n=4$) and 2 months ($n=4$) old female animals. Total node number per each branching degree is shown

Imaging

Alum carmine-stained slides are covered with a coverslip, and the same histoclear media is used as mounting media to image them. Images were acquired on a Nikon SMZ25 brightfield microscope with a Nikon DS-Ri2 stereoscope. For the mammary gland analysis of response to pregnancy hormones [8]$n=4$ whole mount images were analyzed for the 12-day exposure condition, and $n=3$ for the 6-day exposure condition.

Tracing

Brightfield images of whole-mount mammary gland tissue were traced manually using an iPad and Apple Pencil using the Sketch app. The tracing was saved as a separate layer in the object in a white background. Tracings were completed by multiple individuals to remove potential biases in individual tracings. Each layer was then converted separately into a TIF file for use in the NetworkX analysis pipeline.

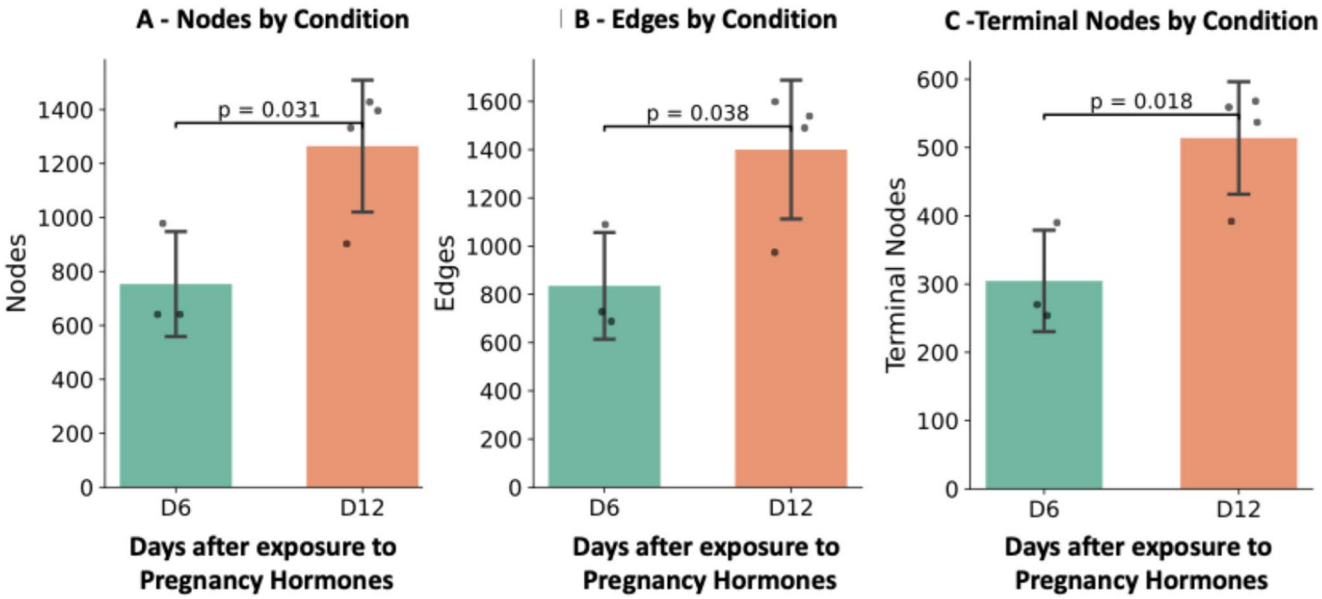

Fig. 5 Utilization of MaGNet for the quantification of whole-mount mammary gland images during hormone-induced pseudo pregnancy. Quantification of the (**A**) number of nodes, (**B**) number of edges, and (**C**) number of terminal nodes from the ductal branching tree in the mammary tissue from female mice exposed to pregnancy hormones for 6 days ($n=3$) or 12 days ($n=4$)

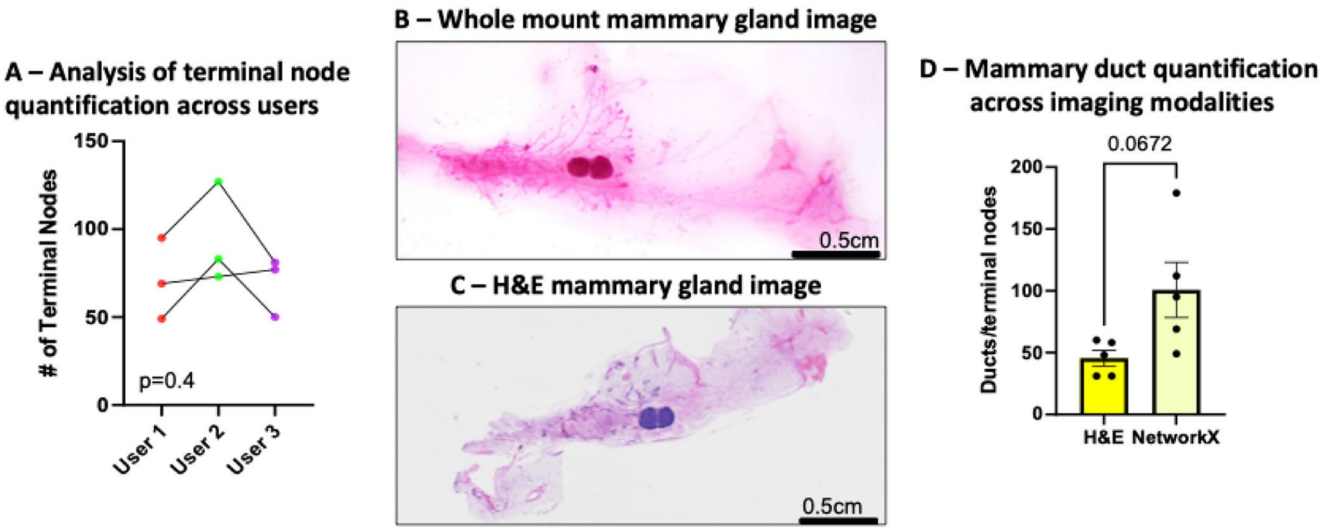

Fig. 6 Validation of MaGNet Analysis Pipeline Performance Through Comparison with Histological Quantification and Assessment of Inter-User Variability. **A** Quantification of terminal nodes tracing of the same whole-mount images by three independent users ($n=3$ users, $n=3$ stained glands each). Each color indicates a different user tracing the same image with lines connecting the different traces from the same image. **B-C** Representative H&E-stained tissue section (**B**) and whole-mount image (**C**) from a 1-month-old female mouse. **D** Quantification of mammary ductal tree via manual duct counts from H&E-stained tissue sections, compared to the network pipeline tracings of whole-mount staining from the same mouse ($n=5$ for each modality from each mouse)

Network extraction from network tracing

Network Extraction From Images (NEFI) was used to go from the manual tracing to the mathematical representation of the network structure [17]. Manual tracings were entered as TIF files. The pre-defined NEFI pipeline 'Leaf Venation' was used to convert the tracing to a network object. Filtering is performed on the main mammary gland object to remove all connected components not belonging to the main connected component.

Analysis of networks characteristics

To analyze and quantify mammary gland network features, we developed a Python pipeline using the NetworkX python package [18]. NEFI networks are used as input in the shape

of the NEFI output.txt text with spatial network coordinates. In our pipeline, a function read_nefi_graph() is defined to transform the NEFI outputs into a NetworkX Python object. The graph can be visualized with the function quick_plot(). The pipeline supports the calculation of different network properties, such as the number of edges (ducts), number of terminal nodes (TEBs), length of edges, normalized length of branching tree by tree area, convex hull area occupied by the ductal network, and analysis of degree branching distribution.

Statistical analyses and data visualization

All statistical analyses and data visualization from raw data were conducted in Python. For statistical analysis between groups, Tukey's HSD tests were performed using the statsmodels function pairwise_tukeyhsd. The Python package Seaborn [23] was used to develop our own functions for data visualization, available on our code.

Acknowledgements This work was performed with assistance from CSHL Animal Facility, and the CSHL Tissue Histology Shared Resources, which are supported by the CSHL Cancer Center Support Grant 5P30CA045508. This work was financially supported by the Pershing Square Sohn Prize for Cancer Research (C.O.D.S.), the CSHL and Simons Foundation Award (C.O.D.S), the CSHL and Northwell Health affiliation (C.O.D.S), the NIH/NCI grant R01CA248158-05 (C.O.D.S.), NIH/NIA grant R01AG069727-05 (C.O.D.S.), the NIH/NCI R01CA284630-3 (C.O.D.S.), the NIH NCI grant F30CA281082 (S.M.L.), the NIHGM T32GM008444 (S.M.L.), and a fellowship from "la Caixa" Foundation (ID 100010434, code "LCF/BQ/EU23/12010061" to L.T.P.).

Author Contributions C.O.D.S. supervised the research; S.M.L., L.T-P., S.H., and C.O.D.S designed the research and wrote the manuscript. S.M.L., L.T-P., and S.H. performed experiments and data analysis. X.Z. and S.N. provided critical support on data analysis.

Data Availability No datasets were generated or analysed during the current study. Code availability: The relevant code for this pipeline has been laid out as an interactive notebook openly available on Google Colab (Mammary gland analysis on NetworkX). Folders with demo data have also been uploaded to Github for users to try out the functionalities (https://github.com/lucia-tellez/NetworkAnalysis/tree/main).

Declarations

Conflict of interest The correspondent author is an EdBoard member for the Journal of Mammary Gland Biology and Neoplasia.

References

1. Hogan BLM. Morphgenesis Cell. 1999;96:225–33.
2. Short KM, Smyth IM. The contribution of branching morphogenesis to kidney development and disease. Nat Rev Nephrol. 2016;12:754–67.
3. Conn A, Pedmale UV, Chory J, Navlakha S. High-Resolution laser scanning reveals plant architectures that reflect universal network design principles. Cell Syst. 2017;5:53–e623.
4. Conn A, Pedmale UV, Chory J, Stevens CF, Navlakha S. A statistical description of plant shoot architecture. Curr Biol. 2017;27:2078–e20883.
5. Hannezo E, et al. A unifying theory of branching morphogenesis. Cell. 2017;171:242–e25527.
6. Fu NY, Nolan E, Lindeman GJ, Visvader JE. Stem cells and the differentiation hierarchy in mammary gland development. Physiol Rev. 2020;100:489–523.
7. Slepicka PF, Cyrill SL, dos Santos CO. Pregnancy and breast cancer: pathways to understand risk and prevention. Trends Mol Med. 2019;25:866–81.
8. dos Santos CO, Dolzhenko E, Hodges E, Smith AD, Hannon GJ. An epigenetic memory of pregnancy in the mouse mammary gland. Cell Rep. 2015;11:1102–9.
9. Hennighausen L, Robinson GW. Information networks in the mammary gland. Nat Rev Mol Cell Biol. 2005;6:715–25.
10. Rusidzé M, et al. Estrogen receptor-α signaling in post-natal mammary development and breast cancers. Cell Mol Life Sci. 2021;78:5681–705.
11. Vandenberg LN, Schaeberle CM, Rubin BS, Sonnenschein C, Soto AM. The male mammary gland: A target for the xenoestrogen bisphenol A. Reprod Toxicol. 2013;37:15–23.
12. Blacher S, et al. Quantitative assessment of mouse mammary gland morphology using automated digital image processing and TEB detection. Endocrinology. 2016;157:1709–16.
13. Scheele CLGJ, et al. Identity and dynamics of mammary stem cells during branching morphogenesis. Nature. 2017;542:313–7.
14. Short K, Hodson M, Smyth I. Spatial mapping and quantification of developmental branching morphogenesis. Dev (Cambridge). 2013;140:471–8.
15. Satta JP et al. Exploring the principles of embryonic mammary gland branching morphogenesis. Dev (Cambridge). 2024;151(15):dev202179.
16. Kessenbrock K, et al. Diverse regulation of mammary epithelial growth and branching morphogenesis through noncanonical Wnt signaling. Proc Natl Acad Sci U S A. 2017;114:3121–6.
17. Dirnberger M, Kehl T, Neumann A. NEFI: network extraction from images. Sci Rep. 2015;5:1–10.
18. Hagberg AA, Schult DA, Swart PJ. Exploring network structure, dynamics, and function using networkX. Proc 7th Python Sci Conf. 2008;11–15. https://doi.org/10.25080/tcwv9851.
19. Hanasoge Somasundara AV, et al. Parity-induced changes to mammary epithelial cells control NKT cell expansion and mammary oncogenesis. Cell Rep. 2021;37:110099.
20. Feigman MJ, et al. Pregnancy reprograms the epigenome of mammary epithelial cells and blocks the development of premalignant lesions. Nat Commun. 2020;11:1–12.

21. Frey WD, et al. BPTF maintains chromatin accessibility and the Self-Renewal capacity of mammary gland stem cells. Stem Cell Rep. 2017;9:23–31.
22. Henry S, et al. Host response during unresolved urinary tract infection alters female mammary tissue homeostasis through collagen deposition and TIMP1. Nat Commun. 2024;1–14. https://doi.org/10.1038/s41467-024-47462-7
23. Waskom M. Seaborn: statistical data visualization. J Open Source Softw. 2021;6:3021.